

Fast Neutron Dose Distribution Measurements inside Water Phantom using LR115 Track Detectors

Adnan N. Rashed

Jeddah Community College

King Abdulaziz University, Jeddah, Saudi Arabia

Adnan96b@hotmail.com

Abstract: Fast neutron fluence and absorbed dose distribution from Am-Be neutron source has been measured inside water phantom using cellulose nitrate (LR-115) solid state nuclear track detector (SSNTD). The absorbed doses calculated using fluence –Kerma Conversion factors have been compared with those calculated by using fast neutron scattering cross sections for Hydrogen and Oxygen. The relaxation length and build up factors have been measured. An empirical formula was proposed for depth dose calculations. Dose equivalent as well as effective dose in each of the various human body tissues are extracted by weighting the measured dose according to the International Commission of Radiological Protection (ICRP) latest published weighting factors.

Keyword: Fast Neutron Depth Dose, LR115 SSNTD, Am-Be neutron source, Absorbed dose, Equivalent Dose, Effective Dose.

1. Introduction

Fast neutrons have the advantage of efficient treating cancer cells with lower doses, regardless of hypoxia (lower oxygen content in tumor than in normal tissues) over the other types of ionizing radiations. That is for their relatively high linear energy transfer (LET) and relative biological effectiveness (RBE). Nowadays, fast neutron therapy is being used to treat cancer efficiently in some human organs^[1-4]. Fast neutron therapy including the use of radionuclides besides radiation protection in medicine, industry and research necessitate an accurate physical dosimetry. Dose distributions from immersed neutron sources are more strongly altered by a combination of several effects such as

backscattered neutrons near the source and attenuation of neutron fluence at greater distances.

The importance of detector material is that its elemental composition by weight, together with the neutron energy spectrum, determines the effective Kerma per unit fluence at the detector. Phantom material and phantom size are also important factors for the incident and scattered neutrons. However, phantom size has been shown to exert little influence on the neutron dose distribution near centrally located ^{252}Cf source in spherical phantoms greater than 10 cm in diameter^[5].

Measurements of the absorbed dose in a tissue equivalent phantom have been carried out by means of ionization chambers^[6,7], silicon diodes^[8,9], thermoluminescence dosimeters^[10], track etching detectors^[11-13], and by activation detectors^[14].

The advantage of tissue equivalent ionization chamber method is the direct tissue equivalent and energy – independent measurement of the absorbed dose; on the other hand its size does not enable doses near the source to be measured. Silicon diodes are not tissue equivalent. However, the use of recoil track detectors enables absorbed dose measurements near the source to be performed.

Although CR-39, Allyl diglycol carbonate ($\text{C}_{12}\text{H}_{18}\text{O}_7$) SSNTD of thickness about $500\mu\text{m}$ shows good performance recently in neutron dosimetry^[15], LR-115 cellulose nitrate is closer to tissue composition than CR-39, and LR-115 threshold is 1MeV that enables them to measure fast neutron doses only, while CR-39 threshold is about 0.05MeV that made them sensitive to slow neutrons also. Nowadays, both LR-115 and CR-39 are used together side by side in radiation dosimetry^[16,17]. However, LR-115 cellulose nitrate ($\text{C}_6\text{H}_7\text{N}_3\text{O}_{11}$ – Approx.) track detector with $12\mu\text{m}$ thick and $Z_{\text{eff}}=7.2$ is a more suitable detector for fast neutron dose measurements at smaller depths with high accuracy and can be considered as a tissue equivalent material.

The aim of the present paper is to investigate the fast neutron fluence and absorbed dose distribution from Am-Be neutron source inside water phantom using LR-115 track detector. The absorbed doses calculated by using fluence – Kerma conversion factors have been also compared with absorbed doses calculated by using the fast neutron scattering cross-sections for hydrogen and oxygen (*i.e.* for H_2O). Also, the expected dose equivalent and effective dose in various human tissues have been shown.

2. Experimental

A 5 Curie Am-Be neutron source was positioned centrally in water phantom. The source is 3cm diameter and 6cm height with an emission rate of 1.1×10^7 neutron/sec. The phantom used is a cylindrical Lucite tank of 60 cm diameter and 80 cm height filled with water, simulating human body, since human body is approximately 70% water, and dose measurement is calculated and calibrated as dose to water. The detector used is LR-115, cellulose nitrate (manufactured by Kodak Pathe- France) with 12 μm thick in a 100 μm plastic base.

The fast neutron sensitivity of LR-115 (to Am-Be) has been determined by free air calibration and etching in 10% NaOH at 60° C for 70 min. The tracks were counted using Karl Zeis microscope. The sensitivity was found to be $(3.37 \pm 0.3) \times 10^{-6}$ track/neutron. During the experimental work, the detectors were maintained at depths in phantom ranging from 0.8 to 18.8 cm, *i.e.* at distances from 2.3 to 20.3cm from the center of the source.

Fluence –Kerma Conversion factor of 4.9×10^{-9} rad.cm²/neutron (*i.e.* 2.041×10^8 n/cm² = 1 rad) [18] has been used. Radiation weighting factor ($W_r = 10$) which is neutron energy dependent, has been used for absorbed dose (Da) conversion to dose equivalent (DE), since $DE = Da \times W_r$. Also, human body tissues weighting factors (W_t) have been used to calculate the effective dose (DT) in each tissue, as $DT = DE \times W_t$. The used values of W_t for the various tissues are as follows: 0.2 for gonads, 0.12 for each of bone marrow, colon, lung, or stomach, 0.05 for each of bladder, breast, liver, Esophagus, or thyroid, 0.1 for each of skin or bone surfaces. Also, for less sensitive tissues, $W_t = 0.005$ for each of adrenals, upper large intestine, small intestine, kidney, muscles, pancreas, spleen, thymus or uterus. The mentioned values of W_r and W_t are the latest recommended weighting factors by ICRP, [19].

The measured fast neutron fluences were those above 1MeV which is the threshold of LR-115 detector. The results presented below are transverse axis data according to the irradiation geometry.

3. Results and Discussion

The fast neutron flux distribution determined by the LR-115 track detectors at various depths in water as well as in free air are represented in Figure 1. Free air irradiations were performed at the same dosimeter positions in the empty phantom. It is clear that fast neutron fluxes decreases by increasing depths. The fluence ratio in water and air (Φ_w/Φ_a) is represented in Figure 2.

The attenuation in phantom (tissue) can be obtained from the following equation:

$$\Phi_w / \Phi_a = B(x). \exp(-x / \lambda) \quad (1)$$

where $B(x)$ is the build-up factor and λ is the relaxation length. The relaxation length evaluated from Fig. 2 is 8.0cm, excluding the variation in the build-up factor $B(x)$ at lower tissue depths. The value of $\lambda = 8.0\text{cm}$ is valid from tissue depths of $\sim 5\text{cm}$ up to 18.8cm. The calculated value of λ is 7.2 as the reciprocal of the linear absorption coefficient of water for neutrons of spectrum similar to Am-Be spectrum^[20]. This calculated value of λ is about 10% lower than that measured in this experiment, because the calculated value has considered a point neutron source. At tissue depths smaller than 5cm, a build up factor $B(x)$ should be considered. From Figure 3, it is clear that $B(x)$ increases with depth from 0.8cm to $\sim 5\text{cm}$ reaching a maximum value of ~ 1.3 at 5cm and then becomes more or less constant. This mentioned value of $B(x)$ goes with the results in the literature,^[12].

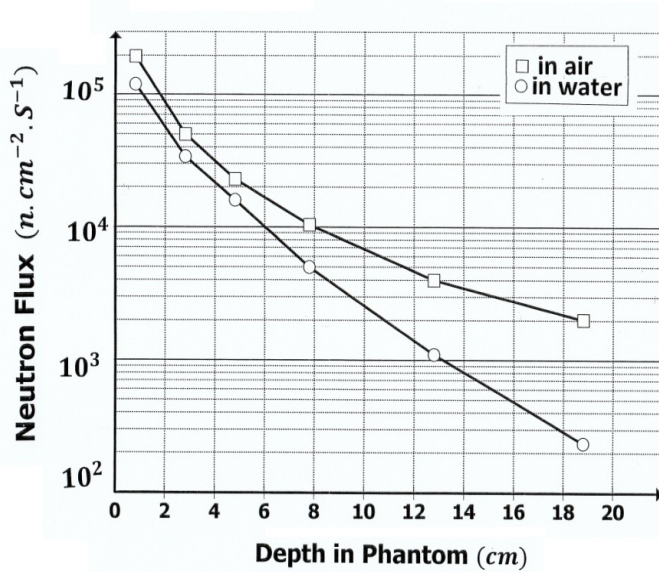


Fig. 1. Fast Neutron flux distribution at various depths.

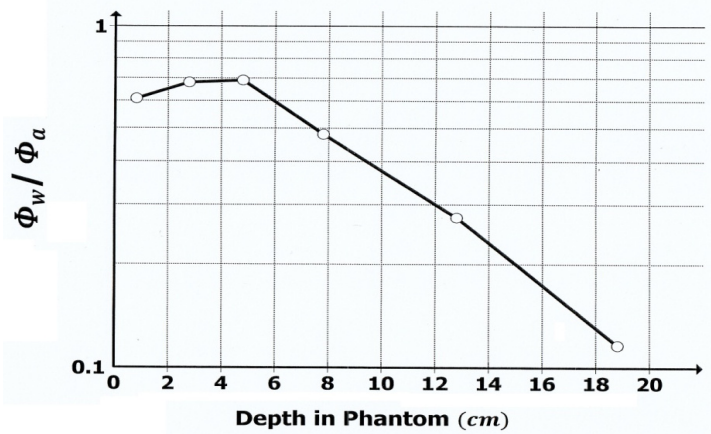


Fig. 2. Fluence ratio in water and in air at various depths.

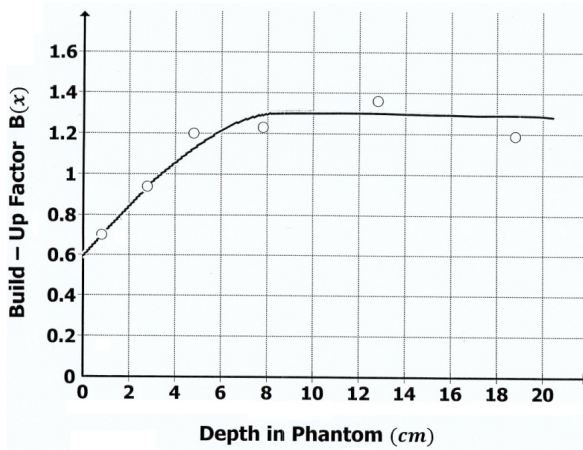


Fig. 3. Variation of build-up factor with depth.

In Figure 4, the variation of absorbed dose rate, as calculated from fluence-Kerma conversion factor in water^[18] with depth in phantom is shown. It is clear that dose rate decreases by increasing depth in phantom. In Figure 4, also the variation of the fast neutron absorbed dose rate $D_a(E)$ vs. depth according to scattering cross-sections is represented too. The latter was calculated using the following formula^[20]:

$$D_a(E) = \frac{(1.6 \times 10^{-13} \text{ (J / MeV)}) \Phi E \sum N_i \sigma_i f_i}{1 \text{ (J / kg.Gy)}} \quad \text{Gy/sec} \quad (2)$$

where Φ is the measured fast neutron flux in ($n/cm^2 \cdot sec$), E is the neutron energy (taken as $5MeV/n$), N_i is the number of atoms per kilogram for hydrogen and oxygen in water (taken as 6.69×10^{25} and 3.345×10^{25} respectively), σ_i is the scattering cross-sections of hydrogen and oxygen (taken as 1.5 barn and 1.55 barn respectively), and f_i is the mean fraction energy transfer to scattered atom (taken as 0.5 and 0.111 respectively). The factor $1(J/Kg \cdot Gy)$ in the denominator comes from the fact that the dose of ($1Gy$) corresponds to the absorption of ($1 J/Kg$) by the target.

It is clear from Figure 4 that both curves (of dose measured in Kerma and the one calculated using Eq. (2)) are in good agreement. This agreement supports the use of LR-115 as a tissue equivalent detector in depth dose measurements. However, the calculated dose, using Eq. (2) is slightly lower in about 8% than the measured one. This is because the calculation in Eq. (2) has been done over a monoenergetic neutron beam of energy 5MeV. It should be averaged over the whole fast neutron Am-Be energy spectrum (i.e. $\sim 1-11 MeV$).

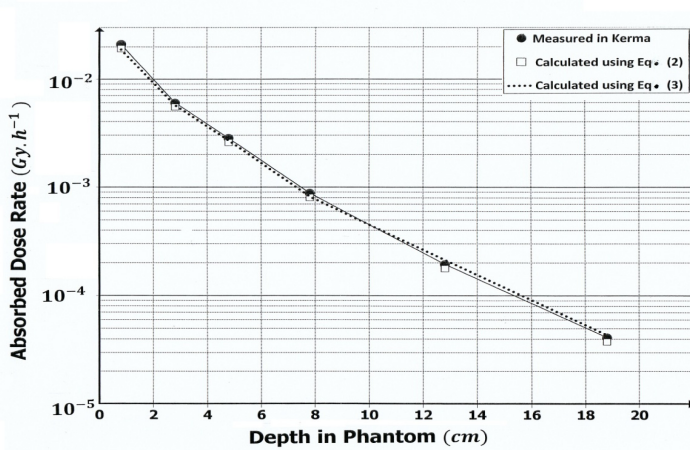


Fig. 4. Absorbed dose rate as a function of depth in phantom

Starting from the inverse square law to calculate the absorbed dose rate D_a in the various depths in phantom (tissue), considering the attenuation of dose with depth, the effect of Build-up factor and relaxation length, an empirical equation can be deduced to calculate the absorbed dose rate D_a . This empirical equation is as follows:

$$D_a = \frac{1.81 \times 10^{-5} \cdot B(x) \cdot \Phi_o \cdot \exp(-x/\lambda)}{4\pi(x+c)^2} \quad \text{Rad/hour} \quad (3)$$

where Φ_0 is the neutron source emission rate, neutron/sec, x and c are the phantom (tissue) and void (noninteracting) depths respectively, $(x + c)$ is the distance from the source center to the detector, λ is the relaxation length (= 8.0 cm), and $B(x)$ is the build – up factor obtained from Figure 3. The graph of the deduced empirical equation - Equation (3), is shown also in Figure 4 as the dotted line.

However, Equation (3) is valid with a tolerance not more than $\pm 10\%$ over the whole range of dose measured at various depths (i.e. from 0.8 cm to 18.8 cm). This slight difference between the measured and the calculated values using Equation (3) of dose rate may be due to the fact that the fluence-Kerma conversion factors used are based on unidirectional broad beam of monoenergetic neutrons at normal incidence; which is not exactly similar to our experiment circumstances. In this experiment, the neutron fluence is of isotropic distribution around the source located in the center of cylindrical phantom, *i.e.* not unidirectional broad beam. Also, the neutron fluence in this experiment is not monoenergetic but of fairly wide spectrum and not with exactly normal incidence on the detector but with a solid angle.

Figure 5 shows the variation of calculated dose equivalent rate (DE) with phantom depths. When the whole human body receives uniformly the dose equivalent (DE) of Figure 5-1, the corresponding values of effective dose in each organ will be as shown in Graph 2-6 of Figure 5, according to the organs tissues sensitivities. The total effective dose is the sum of all partial effective doses (DT) within each tissue that coincide with Figure 5-1 in each phantom depth. In this case, all organs will contribute to the total risk of a health effect, such as cancer. However, in case of internal emitter, only one or two organs will receive the dose while the other organs will not be at risk. But in radiotherapy, the dose value and the tissue size under treatment will be under control.

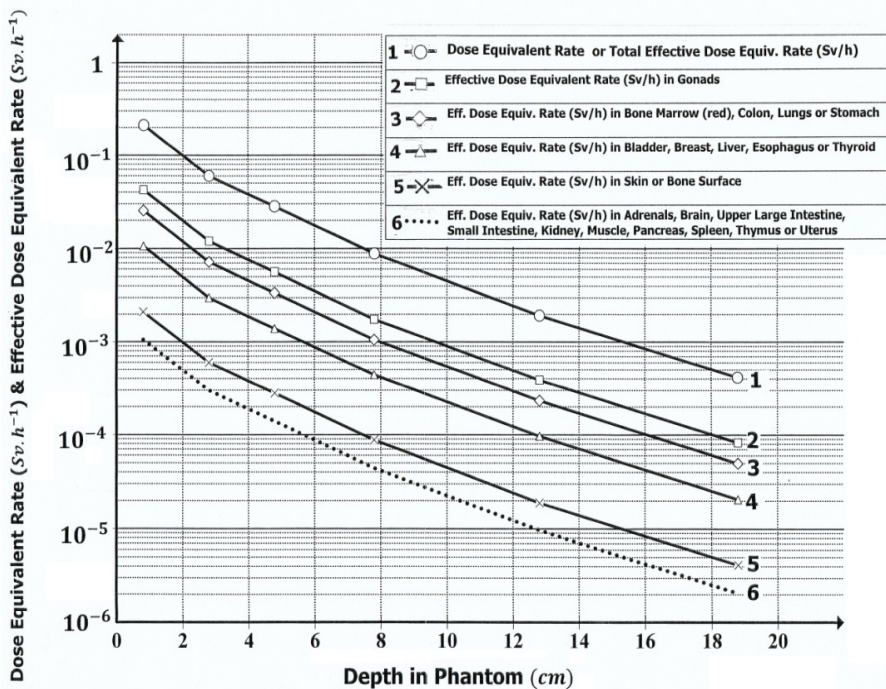


Fig. 5. Dose equivalent and effective dose rates vs. depth in phantom.

4. Conclusion

LR-115 cellulose nitrate detector is used to measure the fluence and depth dose distribution of Am-Be neutron source in water phantom for isotropic distribution. The use of such detector enables measurements in approximately tissue equivalent material at smaller depths. The relaxation length has been found to be 8.0 cm in fair agreement with the calculated one. Below a depth of 5cm, a build up factor should be considered in dose calculation. The absorbed doses calculated through fluence – Kerma conversion factors agreed with those calculated through neutron scattering cross sections. An empirical formula has been deduced for dose rate calculation with high accuracy.

References

- [1] Kononov, V., Bokhovko, M., Kononov, O., Soloviev, N., Chu, N. and Nigg, D. (2006) *Nucl. Instr. Methods Phys. Res., Sec. A*, **564**(1): 525.
- [2] Schwartz, D., Einck, J., Bellon, J. and Laramore, G. (2001) *Int. J. Radiat. Oncology Biol. Phys.*, **50**(2): 449.

- [3] **Laramore, G., Krall, J., Thomas, F., Russell, K., Maor, M., Hendrickson, F., Martz, K., Griffin, T. and Davis, L.** (1993) *Am. J. Clin. Oncol. (CCT)* **16(2)**: 164.
- [4] Booklet of NIU Institute for Neutron Therapy at Fermilab, Illinois, USA, see: www.neutrontherapy.niu.edu
- [5] **Anderson, L.L.** (1973) *Phys. Med. Biol.*, **18**: 779.
- [6] **Lee, D., Ji, Y., Lee, D., Park, H., Lee, S., Lee, K., Suh, S., Kim, M., Cho, C., Yoo, S., Yu, H., Gwak, H. and Rhee, C.** (2001) *J. Korean Soc. Ther. Radiol. Oncol.*, **19(1)**: 66.
- [7] **Greene, D., Major, D. and Meredith, W.** (1972) *Proc. 1st symp on neutron dosimetry in biology and medicine*, **EUR 4896 d-e-f**: 839.
- [8] **Oliver, G.D.** (1968) *PhD thesis, Univer. of Oklahoma.*
- [9] **Bradley, P., Rosenfield, A., Allen, B., Coderre, J. and Capala, J.**(1999) *Radiation Res.*, **151**: 235.
- [10] **Baccaro, S., Cemmi, A., Colombi, C., Fiocca, M., Gambarini, G., Lietti, B. and Rosi, G.** (2004) *Nucl. Instrum. Method in Phys. Research, Sec. B*, **213**: 666.
- [11] **El-Sersy, A., Khaled, N. and Eman, S.** (2004) *Nucl. Inst. Methods Phys. Res. B*, **215**: 443.
- [12] **Moustafa, H., Abdel-Wahab, M., El-Enany, N., El-Fiki, S., Sharaf, M., Mohamed, R. and El Feky, M.** (1991) *Isotopes in Environ. Health Studies*, **27(4)**: 202.
- [13] **Sayed, A. and Kenawy, M.** (1978) *Proc. 6th Euratom symposium on microdosimetry*, Harwood Academic Publishers Ltd, **EUR-6064 DE-EN-FR**: 517.
- [14] **Sayed, A. and Al-Liabi, N.** (1984) *Isotopenpraxis*, **20**: 416.
- [15] **Tsuruta, T.** (2002) *RPA 10- Proc.meetings Forum*, No. P-3b-160, Hiroshima, May.
- [16] **Zunic, Z., McLaughlin, J., Walsh, C. and Benderac, R.** (1999) *Radiat. Meas.*, **31(1-6)**: 343.
- [17] **Dwaikat, N., Safarini, G., El-Hasan, M. and Iida, T.** (2007) *Nucl. Instrum. Methods Phys. Res. Sec. A*, **574(2)**: 289.
- [18] **Vega-Carrillo, H., Manzanares-Acuna, E., Barquero, R., Gutierrez-Villanueva, J. and Martin-Martin, A.** (2007) *Alasbimn Journal Revista de Medicina Nuclear*, **9(37)**: Article No. AJ37- 5, July.
- [19] *ICRP publication No.73*, **26(2)**: 67 (1996), Pergamon press. Also, *ICRP publication No. 60*, (1991).
- [20] **Cember, H.** (1996) *Introduction to health physics*, 3rd Ed., , McGraw-Hill.

قياس توزيع جرعات النيوترونات السريعة في وسط مائي، باستخدام كواشف عد الأثر المصنع من نترات السليولوز

عدنان نعمان راشد

كلية المجتمع بجدة - جامعة الملك عبد العزيز

جدة - المملكة العربية السعودية

Adnan96b@hotmail.com

المستخلص: تم قياس توزيع فيض وجرعات النيوترونات السريعة في وسط مائي (شبيه النسيج الحي)، وذلك باستخدام كواشف عد الأثر من مادة نترات السليولوز. مصدر النيوترونات المستخدم هو أمرشيوم-بريليوم. من نتائج القياس، تم حساب توزيع جرعات النيوترونات الممتصة في الوسط المائي باستخدام تحويل الفيض إلى كيما، وتم مقارنة النتائج مع نتائج تفاعل تطاير النيوترونات بذرات الهيدروجين والأوكسجين المكونة للماء، وقد وجد تطابق ملحوظ بين النتيجتين. ومن ضمن نتائج التجربة، تم حساب عامل مدى الاسترخاء وعامل التراكم للنيوترونات في الوسط المائي المستخدم. كما أنه من التجربة تم استخراج معادلة تجريبية لحساب الجرعات الممتصة عند الأعماق المختلفة للوسط المائي. إضافة لذلك حُسب توزيع الجرعة المكافئة، والجرعة المؤثرة في أنسجة الإنسان، وذلك بالاعتماد على أحدث عوامل التحويل، التي تنبأها المنظمة العالمية للوقاية من الإشعاع.